Semiconductor Physics, Quantum Electronics & Optoelectronics, 2012. V. 15, N 1. P. 48-54.

PACS 42.50.Ct

Ultrafast light-matter interaction in transparent medium

Alexander V. Korovin
V. Lashkaryov Institute for Semiconductor Physics, NAS of Ukraine, 03028 Kyiv, Ukraine
E-mail: korovin@isp.kiev.ua

Abstract. The ultrafast interaction between high power laser light and plasma has been studied theoretically. The theoretical simulations are based on the nonlinear Schrödinger equation taking into account group velocity dispersion, diffraction, self-focusing and multiphoton absorption. The plasma is formed during propagation of femtosecond laser pulse with high input power in transparent medium due to multiphoton ionization process. The induced plasma results in light scattering with formation of multiple cones. It was found that plasma forms cone region that is inverse to cones appearing from scattering of electromagnetic field. The Fourier transformation of temporal-spatial dependences of plasma density demonstrates formation of quasi-periodic structure for plasma waves.

Keywords: light-matter interaction, ultra-short laser pulse, multiphoton process, transparent medium.

Manuscript received 15.12.11; revised version received 05.01.12; accepted for publication 26.01.12; published online 29.03.12.

1. Introduction

In recent decades, extra high peak power laser pulses allowing to obtain the extreme intensity of the electromagnetic field in the focus of an ultra-short laser pulses have led to a variety of new applications as well as atmospheric analysis and remote sensing of molecules [1], supercontinuum generation [2, 3], precise scalpels for delicate eye surgery [4], driving sources for table-top particle accelerators [5], etc. Also, one of the most promising applications of ultrafast lasers is a femtosecond-laser processing of transparent materials such as glasses [6], crystals [7], and polymers [8]. This versatile method allows obtaining arbitrary three-dimensional microstructures using a highly focused femtosecond laser beam through a local change in refractive index of the host material. So, integrated optical components can be directly inscribed into the bulk of transparent materials by translating the sample. In fused silica, different regimes of structural changes can be observed [6] depending mainly on the energy carried by the incident individual laser pulses. At low energies, a homogeneous refractive index increase occurs due to the rapid melting and quenching of the glass. In contrast, at high pulse energies microexplosions create permanent voids in the focal volume. Interestingly, at intermediate energies, birefringent index changes are induced. It has been shown that the anisotropy is caused by self-organized structures with subwavelength periodicity, the so-called nanogratings [9] that are oriented perpendicular to the polarization of the writing beam [10]. Since their discovery, much attention has been given to use nanogratings for the fabrication of microfluidic channels [11]. The control of propagation dynamics, both spatial and temporal, is crucial in these applications. This necessitates a complete understanding of the physical processes that govern the spatio-temporal dynamics of the intense ultra-short pulse in the medium. The theoretical description of laser-induced refractive index changes in the interaction of high-intensity laser pulses with plasma was considered by many authors [12-15]. The spontaneous breakup of highly elliptical laser beams into one- and two-dimensional arrays of light filaments was studied in fused silica [16], where the multiple filamentation process is initiated by random intensity

modulation across the beam "amplitude noise". Besides, formation of filamentation was studied at propagation of 1-ps laser pulses in scattering medium (aqueous suspension of 2-μm polystyrene microspheres) where scattering was introduced through a stochastic diffusion and diffraction term [17]. At present, it is reasonable to say that understanding the interplay of various physical processes over the extensive range of various parameters like input power, pulse width, wavelength and repetition rate is far from complete. This is largely due to the fact that experimental conditions vary widely and models used are not always comprehensive. Thus, the physics of this problem needs further study.

In this paper, the numerical simulations of propagation of ultra-short laser pulse in a transparent medium are presented. The theoretical model of ultrafast light-matter interaction is based on the nonlinear Schrödinger equation with taking into account the group velocity dispersion, diffraction, self-focusing and multiphoton absorption as well as continuity equation for the plasma density. Modelling ultra-fast light-matter interaction was performed in 3D space with the spatio-temporal Fourier transformation of electric field and plasma density for transverse (relatively to laser pulse propagation direction) coordinate. This spatio-temporal Fourier transformation gives us information about light-matter interaction because the peculiarities in such transformation correspond to dispersion curves for quasi-particles appearing at interaction between plasmons and photons. Also, this transformation allows us to observe formation of periodic or quasi-periodic structures.

The paper is organized as follows. After introduction, in Section 2 the fundamentals for theoretical description of ultrafast light-matter interaction were made. In Section 3, the numerical results and discussions for simulation of ultra-short laser pulse propagation in transparent medium (fused silica) are presented. The final conclusions are presented in Section 4.

2. Fundamentals

Modelling light interaction with matter in nonlinear regime could be performed using Maxwell equations with induced current when taking into account optical Kerr effect as well as multiphoton and avalanche ionization. The Maxwell equations in SI units could be read

$$\nabla_{\mathbf{R}} \times \mathbf{H}(\mathbf{R},t) = \frac{\partial \mathbf{D}(\mathbf{R},t)}{\partial t} + \mathbf{J}(\mathbf{R},t),$$

$$\nabla_{\mathbf{R}} \times \mathbf{E}(\mathbf{R},t) = \frac{\partial \mathbf{B}(\mathbf{R},t)}{\partial t},$$

$$\nabla_{\mathbf{R}} \cdot \mathbf{D}(\mathbf{R},t) = \rho(\mathbf{R},t),\ \nabla_{\mathbf{R}} \cdot \mathbf{B}(\mathbf{R},t) = 0, \qquad (1)$$

where the designations are commonly used.

In the case of isotropic media, relation between electric displacement and electric field if taking into account the optical Kerr effect can be written in the time domain as follows

$$\varepsilon \mathbf{E}(t) + \chi^{(3)} \mathbf{E}(t) \int_{-\infty}^{\infty} g(t-t') \mathbf{E}^2(t') dt' = \mathbf{D}(t). \qquad (2)$$

where ε is the permittivity for linear response and $\chi^{(3)}$ is the third-order nonlinear susceptibility, $g(t) = \alpha\delta(t) + (1-\alpha) g_{Raman}(t)$ with $g_{Raman}(t) = \frac{\tau_1^2 + \tau_2^2}{\tau_1^2 \tau_2^2} e^{-t/\tau_2} \sin\left(t/\tau_1\right) U(t)$. Neglecting the Raman response ($\alpha = 1$), Eq. (2) can be rewritten as follows

$$\varepsilon \mathbf{E}(t) + \chi^{(3)} \mathbf{E}(t) \mathbf{E}^2(t) = \mathbf{D}(t). \qquad (3)$$

2.1. Multiphoton and avalanche ionization

The evolution equation for the electron density reads [14]

$$\frac{\partial \rho}{\partial t} = W_{PI}\left(|E|^2\right) + \frac{\sigma}{U_i} \rho |E|^2 - \frac{\rho}{\tau_r}. \qquad (4)$$

where τ_r is the electron recombination time, σ is the coefficient of absorption due to inverse bremsstrahlung that follows from the Drude model, and it could be written as

$$\sigma = \frac{k_0 e^2}{n_0^2 \omega_0^2 \varepsilon_0 \mu_e} \frac{\omega_0 \tau_c}{1 + \omega_0^2 \tau_c^2} = \frac{k_0}{\rho_{at}} \frac{\omega_0 \tau_c}{1 + \omega_0^2 \tau_c^2}, \qquad (5)$$

where $k_0 = n_0\omega_0/c = 2\pi/\lambda$ and ω_0 are the wave number and frequency of the carrier wave, respectively, and n_0 is the medium refractive index in the case of linear response, $\rho_{at} = \varepsilon_0\mu_e (n_0\omega_0/e)^2$ – initial electron density in the valence band, μ_e – reduced electron mass, τ_c – momentum transfer collision time. For usual materials, plasma absorption is a decreasing function while plasma defocusing is an increasing function of τ_c. Thus, the collision time characterizes a balance between plasma absorption and plasma defocusing.

For the high-intense light propagating through dielectric media with photon energy lower than the energy gap in media, the multiphoton ionization gives its contribution to free-electron generation, involving transitions from the valence band to the conduction one through the gap potential. For relatively weak fields, the multiphoton ionization rate from Keldysh's theory for *p*-photon ionization can be approximated by [15]

$$W_{PI}(I) = \sigma_p I^p (\rho_{at} - \rho), \qquad (6)$$

where σ_p is the multiphoton (for *p*-photons) ionization cross section.

The current density for avalanche and multiphoton (p-photons) ionization in frequency domain takes the following form

$$\mathbf{j}_\omega = \sigma_\omega \rho_\omega \mathbf{E}_\omega + \sigma_p U_i \left(\rho_{at} - \rho_\omega\right)\left|\mathbf{E}_\omega\right|^{2(p-1)}\mathbf{E}_\omega . \quad (7)$$

So, the absorbed photons or plasma density generation rates are defined from Eq. (7) in the following form

$$G_\omega = \frac{\mathrm{Re}\left(\mathbf{j}_\omega \cdot \mathbf{E}_\omega^*\right)}{U_i} = \frac{\mathrm{Re}\,\sigma_\omega}{U_i}\rho_\omega\left|\mathbf{E}_\omega\right|^2 + \\ + \sigma_p \left(\rho_{at} - \rho_\omega\right)\left|\mathbf{E}_\omega\right|^{2p} . \quad (8)$$

2.2. Initial conditions

To obtain ultra-intense laser pulse, high focusing is needed. We describe focusing the laser pulse by using linearly polarized Gaussian-like beams. So, the initial electric field for laser pulse propagating along z-axis could be presented in the following form [18]

$$E(\mathbf{r},t) = \frac{\mathcal{E}_0 \phi(t)}{1 + iz/z_R}\exp\left\{i\left(kz - \omega t + \frac{kr^2}{2(z - iz_R)}\right)\right\} + c.c., \quad (9)$$

where $w(z) = w_0\sqrt{1 + (z/z_0)^2}$ is the characteristic transverse size of the beam in z-position and w_0 is the beam waist, $z_0 = n\pi w_0^2/\lambda$ is the Rayleigh range ($2z_0$ is the confocal parameter and $f = (1 + i(z/z_0))^{-1}$ is the curvature of the wave at the distance z from the linear focus), $z - iz_0$ is the complex radius of curvature and $\phi(t) = \sec\mathrm{h}(t/\tau_p)$ or $\phi(t) = \exp\left(-(t/\tau_p)^2\right)$ is the temporal pulse shape with the temporal half-width, τ_p. The typical numerical apertures and beam waists measured with a low intensity femtosecond laser at 800 nm for various objectives could be found in [14]. The input laser power is $P_{in} = E_{in}\sqrt{2/\pi}/\tau_p$, so the light intensity could be read as $E_0^2 = 2P_{in}/\pi w_0^2$.

Generally, the focal spot could be approximated by plane wave while outside of focal spot the spherical harmonics give best approximation. More accurate formula for linearly polarized Gaussian-like beams takes the following form [19] in the case of diffraction angle satisfying the condition $\theta_0 = w_0/z_0 = 2/kw_0 << 1$

$$E_x(r_\perp, z) \approx E_0 f e^{-r_\perp^2/w^2(z)} g(\varphi) \\ e^{i\left[kz + r_\perp^2/(z^2 + z_0^2) - \omega t\right]} + O\left(\theta_0^2\right), \quad (10)$$

$$E_y(r_\perp, z) = 0 , \quad (11)$$

$$E_z(r_\perp, z) \approx -i\theta_0 f \frac{x}{w_0} E_x(r_\perp, z) + O\left(\theta_0^3\right), \quad (12)$$

where $z_0 = kw_0^2/2 = w_0/\theta_0$ – depth of focus in the Rayleigh's range, $g(t) = \sec\mathrm{h}(\varphi/\varphi_0)$ – temporal pulse shape, $\varphi = kz - \omega t$ – phase, $\varphi_0 = \omega\tau_p$ – characteristic pulse width.

2.3. Nonlinear Schrödinger equation

In the framework of paraxial equation approximation, the electric field, $E(x,y,z,t)$, of the pulse propagating along the +z-direction is presented using the envelope function in the form

$$E(x,y,z,t) = \mathcal{E}(x,y,z,t)e^{i(k_0 z - \omega_0 t)} + c.c., \quad (13)$$

where $\mathcal{E}(x,y,z,t)$ is the pulse envelope. For the cases of the slowly-varying envelope approximation, the propagation equation for the pulse envelope can be reduced to the nonlinear Schrödinger (NLS) equation from the wave equation using the well-known arguments [12, 14, 15]. The NLS equation could be extended to include the effects of ionization and the effects of the influence of electron plasma on the pulse envelope and takes the form

$$\frac{\partial \mathcal{E}}{\partial z} = -\frac{i}{2}\beta_2\frac{\partial^2 \mathcal{E}}{\partial t^2} + \beta_3\frac{\partial^3 \mathcal{E}}{\partial t^3} + \\ + \frac{i}{2k_0}\left(1 - \frac{i}{\omega_0}\frac{\partial}{\partial t}\right)\left(\frac{\partial^2}{\partial x^2} + \frac{\partial^2}{\partial y^2}\right)\mathcal{E} + \\ + in_2\frac{\omega_0}{c}\left(1 + \frac{i}{\omega_0}\frac{\partial}{\partial t}\right)\left|\mathcal{E}\right|^2\mathcal{E} - \\ - \frac{\sigma}{2}(1 + i\omega_0\tau_c)\rho\mathcal{E} - \frac{1}{2}\frac{W_{PI}\left(\left|\mathcal{E}\right|^2\right)U_i}{\left|\mathcal{E}\right|^2}\mathcal{E} . \quad (14)$$

Usually, $\mathcal{E}$ is normalized in the way when $\left|\mathcal{E}\right|^2$ equals to the intensity of the pulse in W/cm^2. The terms with coefficients β_2 and β_3 take into account second- and third-order group velocity dispersions (GVD), respectively. The first-order GVD term is vanished for the case of frame of reference moving with the group velocity of the pulse. The subsequent term in the left-hand side is the space-time focusing term in which the transverse Laplacian leads to familiar diffraction effects. The fourth term accounts for third-order nonlinear effects due to the intensity dependent refractive index n_2. Self-focusing in space and self-phase modulation (SPM) in time are direct consequences of this term [14, 15, 20]. The partial time derivative in the term causes self-steepening, which leads to the formation of a shock front in the pulse envelope. While SPM is responsible for symmetric broadening of the pulse spectrum, self-steepening causes an asymmetry in the spectrum [20].

The studies of Chiron *et al.*[12], Couairon *et al.* [14] and Kumagai *et al.* [15] justify retaining only the transverse Laplacian in the space-time focusing term for longer pulse widths, 100 fs or longer, when it is of interest to study only the spatio-temporal dynamics for

pulses that are not in the few cycle limit. For the same reason, we can ignore the third-order GVD, self-steepening and Raman response. So, Eq. (14) can be simplified to the following form

$$\frac{\partial E}{\partial z} = -\frac{i}{2}\beta_2 \frac{\partial^2 E}{\partial t^2} + \frac{i}{2k_0}\left(\frac{\partial^2}{\partial x^2} + \frac{\partial^2}{\partial y^2}\right)E + \\ + in_2 k_0 |E|^2 E - \frac{\sigma}{2}(1 + i\omega_0\tau_c)\rho E - \frac{1}{2}\frac{W_{PI}\left(|E|^2\right)U_i}{|E|^2}E. \quad (15).$$

3. Numerical results and discussions

For simulations, we use the Gaussian pulse laser beam with the operation wavelength equal to 800 nm ($\omega_0 = 2.355$ fs^{-1}) and duration $\Delta\tau$ = 150 fs. In this case, deviation of the frequency is about $\Delta\omega = 1/\Delta\tau = 6.667\cdot10^{-3}$ fs^{-1} (following to the uncertainty relation) that is 0.283% from ω_0. So, we can neglect dispersion in optical constants due to slow frequency dependence in this spectral region. In calculations, we use parameters that are typical for propagation of a high-intense laser pulse in fused silica (FS), and they are presented in Table.

Table. Parameters used in simulations of the propagating ultra-short laser pulse in fused silica.

Name	Value	Notation	Unit
point number for *x* discretization	512	N_x	
point number for *y* discretization	512	N_y	
point number for *t* discretization	256	N_t	
first order dispersion parameter	4.894	β_1	fs/μm
second order dispersion parameter	0.034	β_2	fs^2/μm
refractive index	1.4533	n_0	
non-linear refractive index	$3.75\cdot10^{-16}$	n_2	(W/cm^2)$^{-1}$
initial electron density	$2.1\cdot10^{22}$	ρ_0	cm^{-3}
multiphoton ionization cross section	$9.6\cdot10^{-70}$	σ_6	(W/cm^2)$^{-6}$/s
ionization energy	9	U_i	eV
collision time	20	τ_c	fs
electron recombination time	150	τ_r	fs
reduced electron mass	0.64	μ	m_e
input energy	0.135	I_{input}	μJ
z points number	400	N_z	
z-step	0.25	Δz	μm
pulse waist (for 40× magnitude)	0.7	w_0	μm
distance from linear focus and simulation start position	15	*d*	μm

The spatial distribution of the electric field intensity and plasma density are presented in Fig. 1 for various input laser energies. The calculations were made in 3D space using Eqs. (1) and (4) for data from Table. At each step in the *z*-direction, the electric field envelope is determined from Eq. (1) using the split-step Fourier method [21], while the electron plasma density is obtained by second-order Runge-Kutta integration of Eq. (4). The spatial distributions in Fig. 1 were calculated for the time corresponding to the maximum electric field intensity in a linear regime at the focal spot ($z = 0$ and $t = 0$ correspond to position of this linear focal spot). The space step was chosen equal to 0.065 μm. As we can see, the laser beam is gathered while its intensity reach critical intensity allowing effective multiphoton ionization (in the case of fused silica, it is six-photon ionization). Excited electron plasma leads to reducing the medium refractive index and, as a result, electromagnetic field flows around region with the low optical density. After region with electron plasma, the electromagnetic field is gathered again. With increasing the input laser beam energy, the number of self-steepening (interchanging between flow around and gathering of electromagnetic field) processes is increased, too. Also, we clearly observe multiple cone formation (from Fig. 1 the characteristic cone angles can be determined as 13° for 0.135 μJ, 16° and 6° for 0.675 μJ, and 30°, 16° and 10° for 1.35 μJ) in the electric field intensity at laser power increasing and formation of plasma cone (this cone angle is decreased from 25° down to 20° at input energy increasing) with the vertex of a cone opposite to vertex of a cone for electric field intensity.

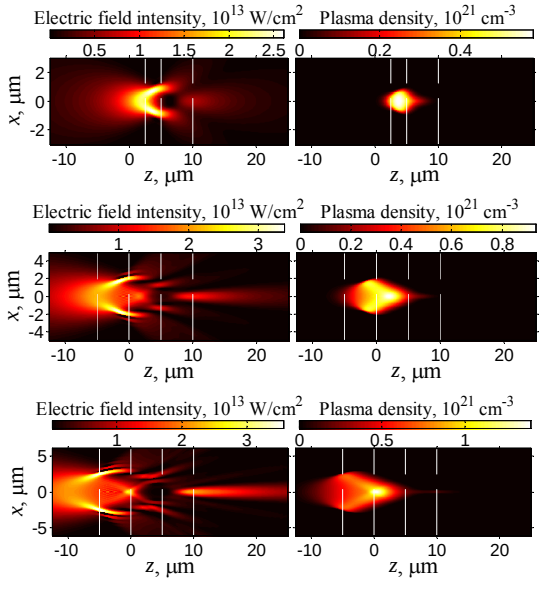

Fig. 1. Spatial distribution of the electric field intensity and plasma density at propagation of an intense light pulse through non-linear medium (fused silica) for various input light energies: 0.135 (a), 0.675 (b) and 1.35 μm (c) and for time corresponding to the electric field intensity maximum in the linear regime at the focal spot ($t = 0$).

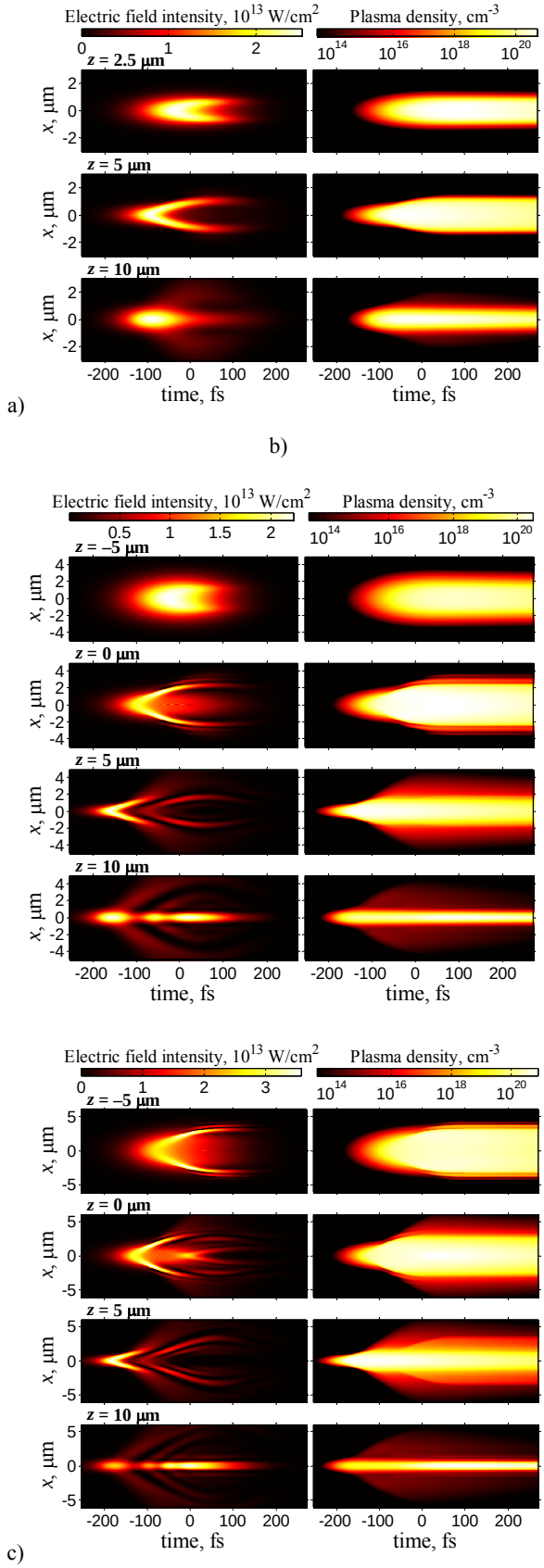

Fig. 2. Time evolution of light intensity and plasma density at z position depicted in Fig. 1 at fixed position $y = 0$ for various input light energies: 0.135 (a), 0.675 (b) and 1.35 μm (c).

The temporal evolution of electric field intensity and plasma density in plane $y = 0$ for laser beam propagation in fused silica at various positions in propagation beam direction corresponding to white dashed lines in Fig. 1 for various input electromagnetic energies are presented in Fig. 2. For the best contrast, the plasma density is presented in the logarithmic scale. Since Eq. (1) is written in the frame of reference moving at the group velocity of the pulse, the real time axis should be shifted by $\beta_1 z$.

This scattering of laser beams in the form of multiple cones is connected with excitation of plasma waves. To proof this, the Fourier discrete transformations (FDT) of the electric field and plasma density over both transverse coordinate and time are presented in Fig. 3. This transformation allowed us to see dispersion relations. Here, we can see formation of a quasi-periodic structure with period about 0.14 μm in the plasma density. Also, Fig. 3 demonstrates formation of plasma waves and such wave could be estimation following to the Bohm–Gross dispersion relation, $\omega_{pl}^2 = \omega_p^2 + (3/2) v_e^2 k_{pl}^2$, where $\omega_p = \sqrt{e^2 n_e / \varepsilon_0 m_e}$ is the plasma frequency, $v_e = \sqrt{2 k_B T_e / m_e}$ – thermal speed of electrons, k_{pl} – electron plasma wave vector, k_B – Boltzmann constant, and T_e – electron temperature. These dispersion curves are presented in Fig. 3 by dashed lines. It was found that the linear plasma response gives us quantitative description of formation of plasma waves in the nonlinear regime. For the case of 0.135 μJ laser pulse, the electron temperature is changed from 10^6 K up to $6 \cdot 10^6$ K with the effective plasma density 10^{18} cm. For the case of 0.675 μJ laser pulse, the electron temperature is changed from $6 \cdot 10^6$ K down to $3 \cdot 10^6$ K with the effective plasma density 10^{18} cm. For the case of 1.35 μJ laser pulse, the electron temperature is changed from $4 \cdot 10^6$ K up to 10^7 K with the effective plasma density 10^{19}, 10^{18} and $4 \cdot 10^{18}$ cm. These values agree in their order with the estimations made in [9] and corresponding periodicity in plasma density is about 0.14 μm. For periodic structure the Brillouin zones are shown by dashed-dotted lines in Fig. 3 for FDT of plasma density. The peculiarities in FDT of electric field intensity could be estimated using the dispersion relation for light waves propagating in electron plasma (bulk plasmon polaritons): $\omega_{pl}^2 = \omega_p^2 + (c/n) k_{pl}^2$, where k_{ph} is the light wave vector and n – plasma refractive index. These dispersion waves are presented in Fig. 3 by solid lines. For the FDT of electric field intensity in Fig. 3, the value of wave vector could be obtained from $k_x = k_{ph} \sin\theta$, where θ is the angle between k_x and k_z components of the wave vector. For fitting, we used 15° angle that corresponds to the angle between cone generatrices and laser beam propagation direction. Also, there are some lines with constant wave vectors in FDT of the electric

field intensity with unknown nature. The corresponding lengths for these lines are 0.23, 0.17 and 0.14 μm and they still unchangeable in the case of input energy changing (dotted lines in Fig. 3).

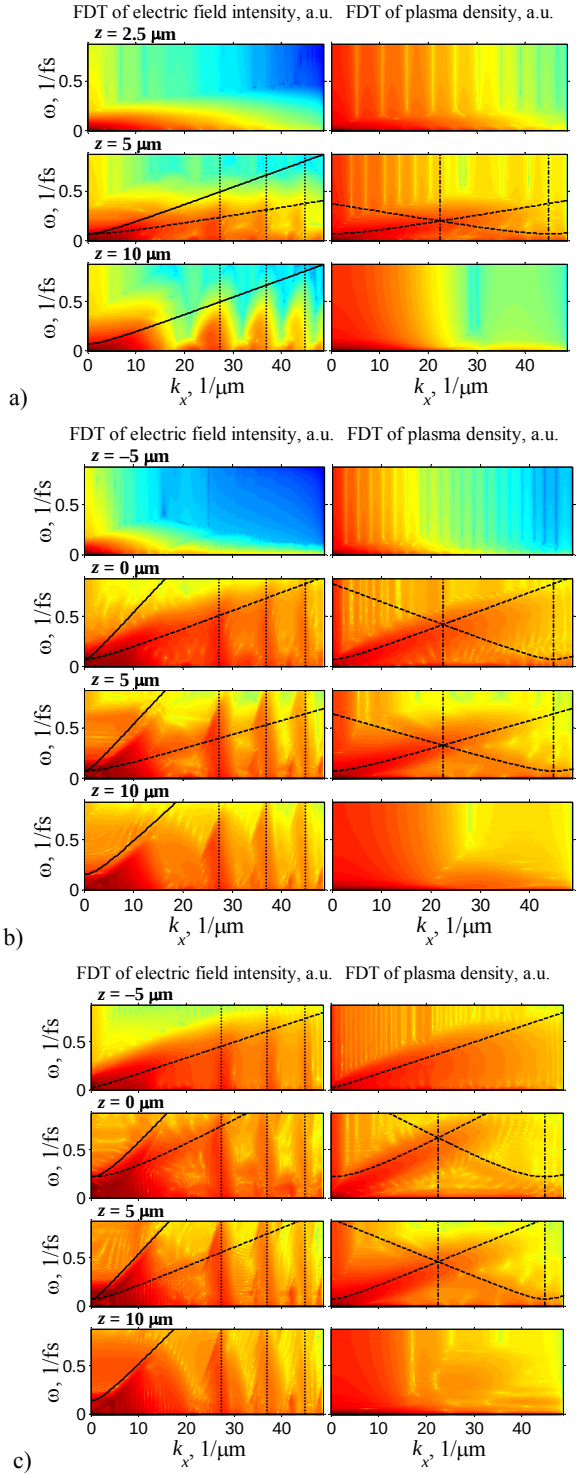

Fig. 3. Coordinate-time Fourier discrete transformation for electric field and plasma density from Fig. 2. Dashed lines correspond to dispersion dependences for surface waves, solid lines – for bulk plasmon polaritons, and dashed-dotted lines – Brillouin zones.

4. Conclusions

In this paper, propagation of an ultra-short laser pulse (150 fs) in transparent medium (fused silica) has been studied in regime of high input powers (0.135, 0.675 and 1.35 μJ) using the nonlinear Schrödinger equation with taking into account the group velocity dispersion, diffraction, self-focusing (optical Kerr effect) and absorption for multiphoton and avalanche ionization processes as well as continuity equation for the electron plasma density. The dynamic of interaction between the laser pulse and electron plasma that is induced by this pulse demonstrates complicated nature of ultrafast light-matter interaction, where competition between self-focusing and plasma defocusing processes leads to formation of multiple cones for the electric filed intensity and single cone formation for the plasma density. Also, the Fourier transformations of spatio-temporal dependences for the electric field and plasma density demonstrate formation of a quasi-periodic structure for plasma waves, which could help in describing self-grating formation. Also, these Fourier transformations demonstrate formation of plasma waves and polaritons that could be estimated by using the linear response approximation.

Acknowledgements

The author gratefully acknowledges financial support by the Deutsche Forschungsgemeinschaft (priority programme 1327 “Optically induced sub-100 nm structures for biomedical and technological applications”).

References

1. J. Kasparian, M. Rodriguez, G. Méjean, J. Yu, E. Salmon, H. Wille, R. Bourayou, S. Frey, Y.-B. André, A. Mysyrowicz, R. Sauerbrey, J.-P. Wolf, and L. Wöste, White-light filaments for atmospheric analysis // *Science*, **301**, p. 61 (2003).
2. V.P. Kandidov, S.A. Shlenov, O.G. Kosareva, Filamentation of high-power femtosecond laser radiation // *Quantum Electronics*, **39**, p. 205-228 (2009).
3. N.K.M. Naga Srinivas, S. Sree Harsha and D. Narayana Rao, Femtosecond supercontinuum generation in a quadratic nonlinear medium (KDP) // *Opt. Express*, **13**, p. 3224 (2005).
4. I. Ratkay-Traub, T. Juhasz, C. Horvath, C. Suarez, K. Kiss, I. Ferincz, R. Kurtz, Ultra-short pulse femtosecond laser surgery // *Ophthalmol. Clin. North. Am.* **14**, p. 347 (2001).
5. S.P.D. Mangles, C.D. Murphy, Z. Najmudin, A.G.R. Thomas, Monoenergetic beams of relativistic electrons from intense laser plasma interactions // *Nature*, **431**, p. 535 (2004).

6. K. Itoh, W. Watanabe, S. Nolte, C. Schaffer, Ultrafast processes for bulk modification of transparent materials // *MRS Bull.* **31**, p. 620-625 (2006).
7. J. Thomas, M. Heinrich, J. Burghoff, S. Nolte, A. Ancona, A. Tünnermann, Femtosecond laser-written quasi-phase-matched waveguides in lithium niobate // *Appl. Phys. Lett.* **91**, 151108 (2007).
8. C. Wochnowski, Y. Cheng, K. Meteva, K. Sugioka, K. Midorikawa, S. Metev, Femtosecond-laser induced formation of grating structures in planar polymer substrates // *J. Opt. A,* **7**, p. 492 (2005).
9. Y. Shimotsuma, P. Kazansky, J. Qiu, K. Hirao, Self-organized nanogratings in glass irradiated by ultra-short light pulses // *Phys. Rev. Lett.* **91**, 247405 (2003).
10. J.D. Mills, P.G. Kazansky, E. Bricchi, J.J. Baumberg, Embedded anisotropic microreflectors by femtosecond laser micromachining // *Appl. Phys. Lett.* **81**, p. 196 (2002).
11. C. Hnatovsky, R. Taylor, E. Simova, P.P. Rajeev, D.M. Rayner, V.R. Bhardwaj, P. Corkum, Fabrication of microchannels in glass using focused femtosecond laser radiation and selective chemical etching // *Appl. Phys. Lett.* **84**, p. 47 (2006).
12. Ram Gopal, V. Deepak and S. Sivaramakrishnan, Systematic study of spatiotemporal dynamics of intense femtosecond laser pulses in BK-7 glass // *Pramana – J. Phys.* **68**, p. 547-569 (2007).
13. A. Chiron, B Lamouroux, R. Lange, J.F. Ripoche, M. Franco, B. Prade and G. Bonnaud, Numerical simulations of the nonlinear propagation of femtosecond optical pulses in gases // *Eur. Phys. J. D,* **6**, p. 383-396 (1999).
14. A. Couairon, L. Sudrie, M. Franco, B. Prade, and A. Mysyrowicz, Filamentation and damage in fused silica induced by tightly focused femtosecond laser pulses // *Phys. Rev. B*, **71**, 125435 (2005).
15. Hiroshi Kumagai, Sung-Hak Cho, Kenichi Ishikawa, Katsumi Midorikawa, Masatoshi Fujimoto, Shinichiro Aoshima, and Yutaka Tsuchiya, Observation of the complex propagation of a femtosecond laser pulse in a dispersive transparent bulk material // *J. Opt. Soc. Am. B,* **20**, p. 597-602 (2003).
16. D. Majus, V. Jukna, G. Valiulis, and A. Dubietis, Generation of periodic filament arrays by self-focusing of highly elliptical ultra-short pulsed laser beams // *Phys. Rev. A,* **79**, 033843 (2009).
17. V. Jukna, G. Tamošauskas, G. Valiulis, M. Aputis, M. Puida, F. Ivanauskas, A. Dubietis Filamentation of ultrashort light pulses in a liquid scattering medium // *Appl Phys. B,* **94**, p. 175-179 (2009).
18. R.L. Sutherland, *Handbook of Nonlinear Optics*. Dekker, New York, 1996.
19. Kirk T. McDonald, Axicon Gaussian Laser Beams // [arXiv:physics/0003056v2 [physics optics] Apr 2000].
20. G.P. Agarwal, in: *The Supercontinuum Laser Source*, ed. by R.R. Alfano. Academic Press, San Diego, 1989.
21. G.P. Agarwal, *Applications of Nonlinear Fiber Optics* (2nd Edition). Elsevier, 2008.